Appendix II

Confirmatory Debris Generation Analyses

The Nuclear Energy Institute (NEI) guidance contains recommendations that will determine the quantities of insulation debris generated with the zone of influence (ZOI). These recommendations include the size of the ZOI based on the insulation destruction pressure and the fraction of the insulation located within the ZOI that subsequently is damaged into the small-fine-debris category. Confirmatory research ascertained whether the NEI recommendation would reliably result in conservative estimates for the volumes of debris generated within the ZOI. This appendix documents the confirmatory research estimates for the volumes of small fine debris. Appendix I covers the confirmatory research for determining the size of the ZOI. Both the NEI guidance and the confirmatory research used the American National Standards Institute (ANSI)/American Nuclear Society (ANS)-58.2-1988 standard to calculate the jet isobar volumes with very similar results. The confirmatory research issues addressed herein include the following:

- The NEI guidance recommends the assumption that 60 percent of the fibrous and 75 percent of the reflective metal insulation (RMI) volume contained within the ZOI become small fine debris. The confirmatory research integrated the insulation damage versus jet pressures over the ZOI volume to determine the fraction of the insulation within the ZOI that would become small fine debris based on available debris generation data.
- The NEI guidance recommends adapting the debris-size distribution for NUKON™ to other types of fibrous insulation that have a destruction pressure higher than that of NUKON™. The size distribution confirmatory research provides partial justification that supports that NEI recommendation.
- The applicability of air-jet-determined destruction pressures to two-phase pressurized water reactor (PWR) loss of coolant accident (LOCA) jets has been questioned. Volume 3 of NUREG/CR-6762 noted that data from the Ontario Power Generation (OPG) two-phase debris generation tests indicate that the destruction pressure could be lower for a two-phase jet than for an air jet and that the resultant debris could be finer. Therefore, it may be prudent to apply a safety factor to accommodate the uncertainty. This confirmatory analysis estimates the volume fractions for small fine debris if an alternate lower destruction pressure were used than those in the NEI guidance.

II.1 Comparison of Jet Isobar Volume Calculations

Three calculations of the jet isobar volumes were available for comparison:*

* The volumes are actually presented in terms of the break diameter cubed (D^3) corresponding to an equivalent spherical radius in terms of r/D (i.e., $4\pi/3\ r^3/D^3$).

(1) the volumes determined from the NEI guidance recommended values for ZOI radii versus the destruction pressures in Table 3-1 of the NEI baseline guidance, where the destruction pressure represents the jet isobar pressure for each particular ZOI radii,

(2) the volumes determined from the confirmatory research (Appendix I) for the ZOI radii versus the jet pressure,

(3) the volumes determined from the Boiling Water Reactor Owners Group (BWROG) recommendation documented in their utility resolution guidance (URG).

Although the volumes in item (3) above apply to a BWR steam jet rather than a PWR two-phase jet, the volumes are compared here to demonstrate the differences between PWR and BWR LOCA jets.

Both the NEI guidance and the confirmatory research volume calculations used the ANSI/ANS-58.2-1988 standard method, whereas the BWROG URG method used the computational fluid dynamics (CFD) code, NPARC, to evaluate the volumes. Figure II-1 compares the equivalent spherical radii for these three methods.

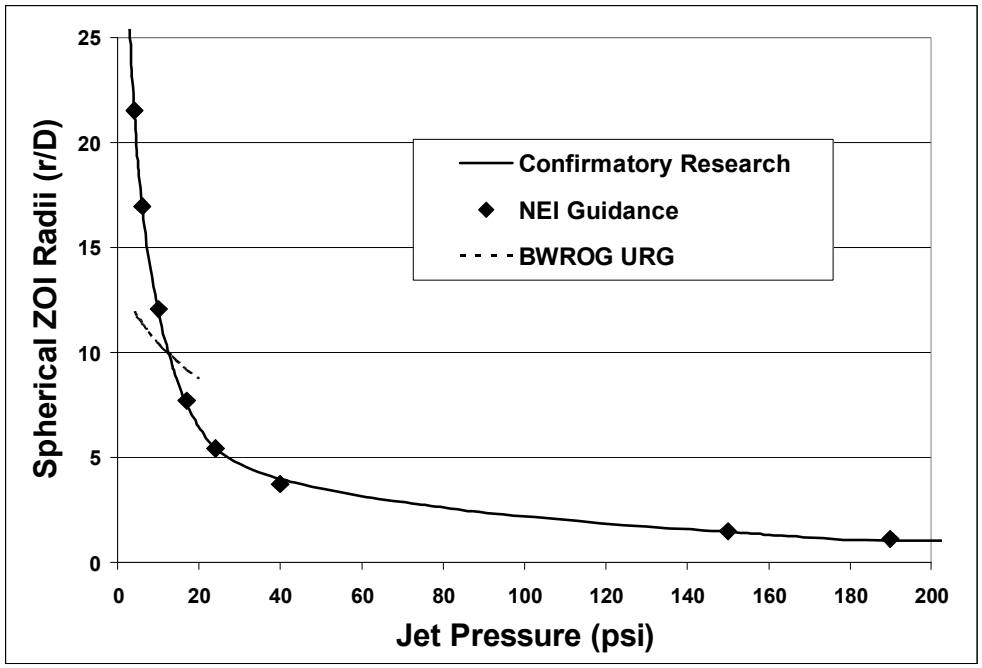

Figure II-1. Comparison of Jet Isobar Volumes

As shown, at the lower jet pressures, the pressure isobar volumes are much larger for the PWR two-phase LOCA jet than for the BWR steam jet. A principal reason for this difference is the higher energy associated with the higher pressure of a PWR reactor coolant system (RCS) than with a BWR RCS; however, another consideration is the accuracy of the ANSI/ANS-58.2-1988 standard at the lower pressures. For example, the validity of the assumption in the ANSI/ANS-58.2-1988 standard that the jet expands at a

half angle of 10 degrees once the jet expansion has reached the asymptotic plane becomes more important at the lower expansion pressures. The accuracy of the debris volumes of insulations that damage significantly at the lower jet pressures is subject to the accuracy of this assumption. Note that the confirmatory research and NEI-recommended-equivalent spherical ZOI radii are in good agreement.

II.2 Method of Determining ZOI Debris-Size Distributions

The volume of debris generated within a ZOI depends on (1) the size of the ZOI defined by the spherical radius, (2) the concentration of a particular insulation within the ZOI, and (3) the fraction of the ZOI insulation that is damaged into a particular debris-size classification. The size distribution and spherical ZOI radius are interdependent. The threshold damage pressure and the jet volumes determine the size of the ZOI (Appendix I). Plant-specific information (i.e., the volume of a particular insulation within the ZOI divided by the volume of the ZOI) determines the insulation concentration within a ZOI.

Integration of experimental debris generation data is required to determine the fraction of the ZOI insulation that is damaged into a particular debris-size classification (e.g., NEI small fine debris). For this integration, NUREG/CR-6808 offered a generalized equation. A slightly expanded version of this equation is

$$F_{ZOI} = \frac{3}{r_{ZOI}^3} \int_0^{r_{ZOI}} f_d\left(P_{jet}(r)\right) r^2 \, dr \quad ,$$

where

F_{ZOI} = the fraction of the ZOI insulation type i that is damaged into a particular debris-size classification,

f_d = the fraction of debris damaged into a particular debris size as a function of the jet pressure P_{jet}, which is a function of the spherical radius, r, within the ZOI, and

r_{ZOI} = the outer radius of the ZOI.

Implicit in this integration is the assumption that the insulation is uniformly distributed within the ZOI, which may not be realistic. Because the functional information needed for this integration is not available in an equation form simple enough for a formal integration to proceed, the following simplification is used,

$$F_{ZOI} = \frac{1}{r_{ZOI}^3} \sum_j \left[\frac{f_{fines}\left(P_{jet}\left(r_j\right)\right) + f_{fines}\left(P_{jet}\left(r_{j-1}\right)\right)}{2} \left(r_j^3 - r_{j-1}^3\right) \right] \quad ,$$

where

f_{fines} = the fraction of debris damaged into a particular debris size as a function of the jet pressure P_{jet} at a radius of r_j.

The spherical ZOI is first subdivided into numerous spherical shells (j). The precision of the integration increases with the number of subdivisions. In a spreadsheet, the jet pressure is listed in increasing values and then the spherical radii are determined, followed by the damage fraction evaluated at each r_j. For the intervals, the average damage across the interval and the volume of the interval are determined. Multiplying the average interval damage by the interval volume, summing, and dividing by the total ZOI volume results in the debris fraction for the ZOI.

II.3 Evaluation of Debris-Specific Damage Fractions and Potential Debris Volume

Potential debris volumes were calculated for fibrous, RMI, and particulate debris types and compared with the NEI baseline model to determine whether the baseline is conservative. The potential volume of debris is defined as the fraction of the ZOI debris damaged into a particular debris size multiplied by the total volume of the sphere, as

$$V_{Potential} = F_{ZOI} \left(\frac{4}{3}\pi \right) r_{ZOI}^3 \quad .$$

Note that to calculate the volume of small fine debris generated, the potential volume must be multiplied by the concentration of insulation ($C_{insulation}$) (i.e., the fraction of the ZOI actually occupied by the insulation) and by the pipe break diameter cubed. Again, it is assumed that the insulation type in question is uniformly distributed over the ZOI, regardless of the size of the ZOI, as

$$V_{Fines} = C_{Insulation} \, V_{Potential} \, D^3 \quad .$$

II.3.1 Fibrous Debris

The fibrous insulation types evaluated include NUKON™, Transco (Transco Products, Inc., or TPI), Temp-Mat, K-wool, and Knauf. Table II-1 shows the destruction pressures recommended in the NEI guidance and an alternate set of values used herein to test the sensitivity of the potential debris volumes to the destruction pressures.

Table II-1. Fibrous Insulation Destruction Pressures

Insulation	NEI Recommendation	Alternate Lower Pressure
NUKON™	10 psi	6 psi
TPI	10 psi*	6 psi
Knauf	10 psi	6 psi
Temp-Mat	17 psi	10 psi
K-wool	40 psi	17 psi

* NEI guidance considers TPI fiber blankets to behave similarly to NUKON™ blankets.

II.3.1.1 Low-Density Fiberglass Debris

A review of the air jet testing debris generation data, both the BWROG air jet impact testing (AJIT) data (BWROG URG) and the drywell debris transport study (DDTS) data (NUREG/CR-6369, 1999), demonstrates that NUKON™, TPI, and Knauf fiberglass insulations underwent similar damage. These insulations have approximately the same as-manufactured density (approximately 2.4 lb/ft^3), and their recommended minimum pressures for destruction are usually taken to be the same pressure. Therefore, these insulations have been grouped together as low-density fiberglass (LDFG) insulation.

Figure II-2 plots the fractions for the small fines from the AJIT debris generation test data as a function of the jet centerline pressure for these three types of LDFG insulations. A curve drawn through the data represents the damage as a function of jet pressure for use in the damage integration over the ZOI. One set of seven data points was from tests (in the DDTS) that used a 4-in. nozzle, whereas the remainder used a 3-in. nozzle. The 4-in. nozzle data from the DDTS generally shows more damage than do the 3-in. nozzle tests. In general, the higher damage occurred because the larger diameter jet exposed more of the target insulation blanket to higher pressures. Note that the data were correlated by the estimated jet centerline pressure, but the pressure on the blanket decreased outward from the centerline. When the blanket was placed close to the jet, the ends of the blanket were hit with substantially less force of flow than the centerline for which the data were correlated. For example, the 3-in. nozzle data point for NUKON™ at a jet pressure of 20 psi damaged only approximately 7 percent of the insulation into small fine debris, whereas this pressure totally destroyed the TPI blankets in the 4-in. nozzle. Apparently, testing blanket destruction for insulations requiring a pressure higher than approximately 17 psi requires a jet nozzle larger than 3 in. For LDFG, any jet pressure larger than 17 psi will totally destroy the blanket into small fine debris, whereas the NEI guidance cited an OPG two-phase jet test with 52 percent of the insulation damaged into small fine debris as its basis of conservatism.

Another significant point of discussion is that the threshold of damage for LDFG insulation has been specified as 10 psi, where Figure II-2 clearly shows damage at jet pressures less than 10 psi. Apparently, neglecting the tail of the damage curve was considered acceptable for the BWR strainer resolution because of the lesser BWR jet volumes at lower pressures, as shown in Figure II-1. However, the much larger jet volumes below 10 psi for the Confirmatory Research/NEI Guidance PWR jet shown in Figure II-1 make the neglect of the tail less acceptable.

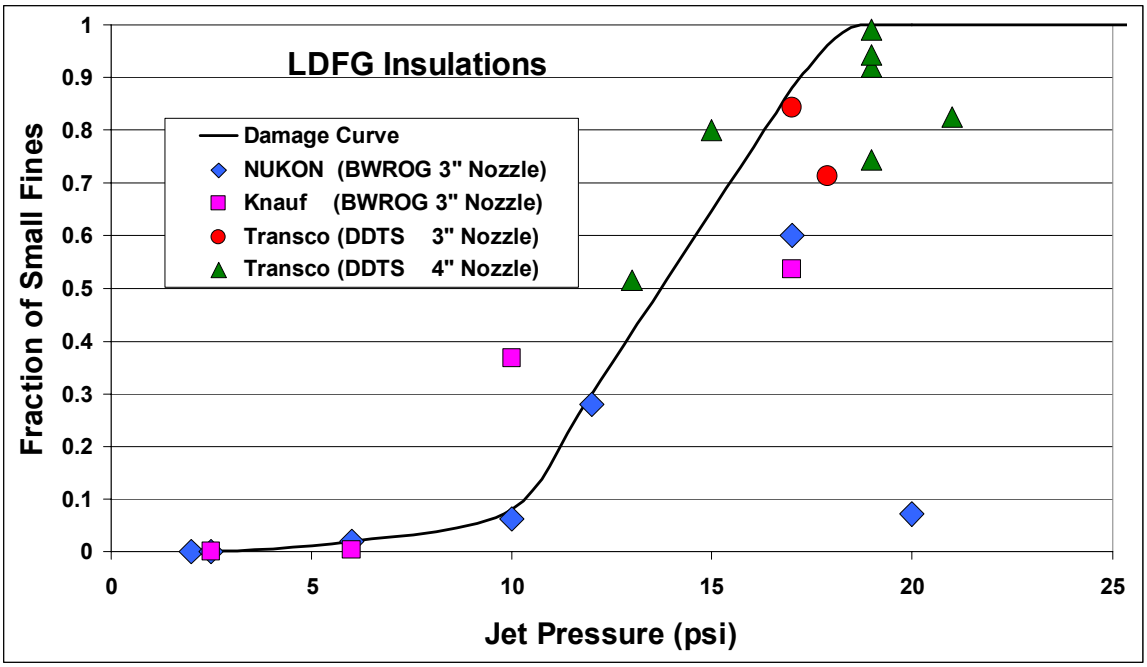

Figure II-2. LDFG Damage Curve for Small Fine Debris

Table II-2 provides the results of debris-size distribution integration over the ZOI. A lower alternate damage pressure results in a larger equivalent spherical ZOI; however, a lesser fraction of the debris is damaged into small fine debris. The use of the alternate damage pressures over the NEI-recommended damage pressures for PWR analyses would result in approximately 16 percent more small fine debris. Figure II-3 compares the potential debris volumes and provides an estimate using the baseline guidance. The baseline estimate is simply 60 percent of $4\pi/3\ (12.1/D)^3$. As shown, the baseline guidance appears to be conservative, but not overly so.

Table II-2. Results of Debris-Size Distribution Integration for LDFG Insulations

Jet Pressure Isobar Volume Calculation	Radius of Sphere (r/D)	Fraction Small Fines	Potential Debris Volumes (V/D^3)
NEI-Recommended Damage Pressures			
BWROG Steam Jet	10.4	0.83	3910
PWR Two-Phase Jet (Confirmatory)	11.9	0.53	3790
Alternate Damage Pressures			
BWROG Steam Jet	11.4	0.65	3980
PWR Two-Phase Jet (Confirmatory)	17.0	0.22	4410

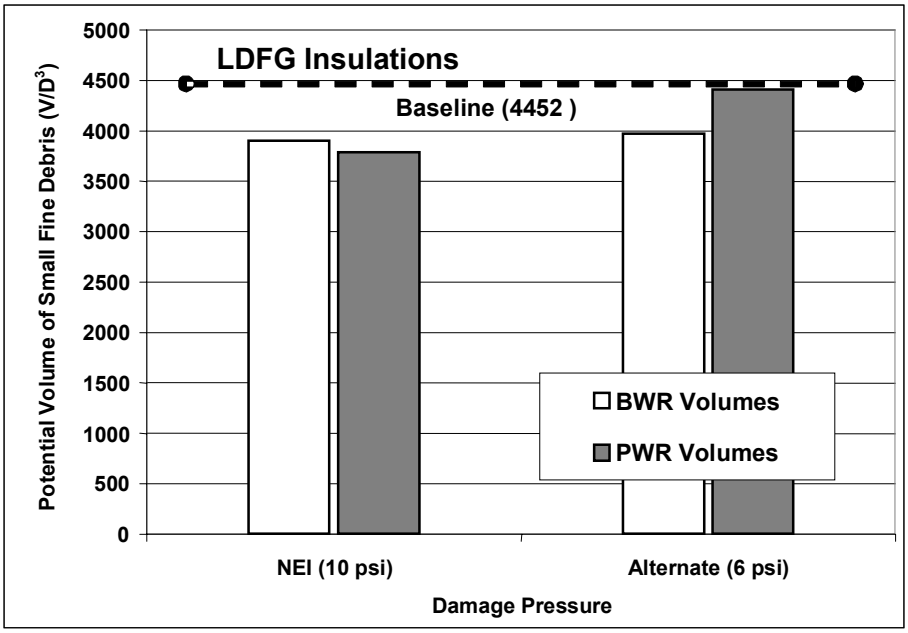

Figure II-3. Potential Volumes of Small Fine LDFG Debris

The NEI baseline guidance completely neglects the transport of large debris to the sump screen; however, some plants will likely need to consider large debris transport as part of a more realistic evaluation. Therefore, the following equation estimates the volume of large debris generated within the ZOI:

$$V_{Large} = C_{Insulation} \left(1 - F_{ZOI}\right) \left(\frac{4}{3}\pi\right) r_{ZOI}^{3} \; D^{3} \quad .$$

In addition, plants that must perform more realistic evaluations may need to subdivide the baseline small-fine-debris class into fines and small-piece debris, where the fines (e.g., individual fibers) remain suspended in the pool and the small-piece debris sinks to the pool floor, where the debris may or may not transport to the sump screen. The baseline guidance has the inherent assumption that all of its small fine debris essentially remains suspended.

In the debris generation tests conducted during the DDTS, 15 to 25 percent of the debris from a completely disintegrated TPI fiberglass blanket was classified as nonrecoverable. The nonrecoverable debris either exited the test chamber through a fine-mesh catch screen or deposited onto surfaces in such a fine form that it could not be collected by hand (it was collected by hosing off the surfaces). Therefore, it would be reasonable to assume that 25 percent of the baseline small fine debris (i.e., F_{ZOI}) is in the form of individual fibers and that the other 75 percent is in the form of small-piece debris.

II.3.1.2 Temp-Mat Debris

Temp-Mat is much higher density insulation (approximately 11.8 lb/ft^3) than the LDFG insulation and requires a significantly higher jet pressure to damage the insulation.

Figure II-4 shows the Temp-Mat insulation debris fractions for the small fine debris from the AJIT tests. This figure shows six data points for Temp-Mat, two of which represent tests where no significant damage was noted. The test with the maximum damage had approximately 36 percent of the insulation damaged into small fine debris, with the remainder of the insulation forming large-piece debris. Unfortunately, no tests were conducted with jet pressures high enough to complete the damage curve to total destruction into small fine debris, as was done for the LDFG insulations. Therefore, a conservative extrapolation of the data is required to perform the debris generation integration over the equivalent ZOI sphere. Figure II-4 shows the extrapolation used herein as a dashed line. Figure II-4 also illustrates the selection of the NEI-guidance damage pressure of 17 psi, where it is seen that significant small fine debris is generated at jet pressures below 17 psi.

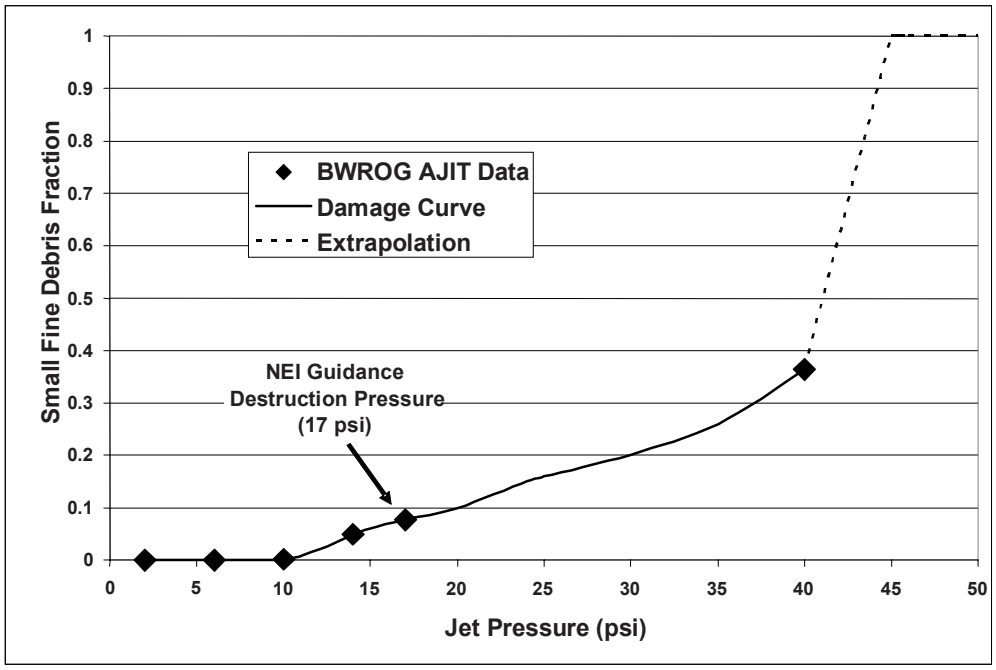

Figure II-4. Temp-Mat Damage Curve for Small Fine Debris

Table II-3 provides the results of the Temp-Mat debris-size distribution integration over the ZOI. Figure II-5 compares the potential debris volumes and provides an estimate using the baseline guidance (60 percent of $4\pi/3\ (7.8/D)^3$). A lower alternate damage pressure results in a larger equivalent spherical ZOI; however, a lesser fraction of the debris is damaged into small fine debris. The use of the alternate damage pressures over the NEI-recommended damage pressures for PWR analyses would result in approximately 36 percent more estimated small fine debris. For Temp-Mat insulation, the baseline is conservative with respect to both the NEI-guidance damage pressure of 17 psi and the alternate pressure of 10 psi.

The debris-size estimate for Temp-Mat has more uncertainty associated with the estimate than does the similar calculation for LDFG, primarily because of more limited data. The negative uncertainties include the neglect of the damage curve tail by the

NEI-recommended damage pressure (quantified using the alternate damage pressure) and the fact that the BWROG AJIT tests used the small 3-in. nozzle, which makes it difficult to subject the entire target blanket to the characteristic jet pressure (near the centerline pressure) when the blanket is located close to the nozzle. The positive uncertainty is the sharp extrapolation of the damage curve to 100 percent destruction at 45 psi. In this case, it is possible that the positive uncertainty overshadows the negative uncertainties.

Table II-3. Results of Debris-Size Distribution Integration for Temp-Mat Insulation

Jet Pressure Isobar Volume Calculation	Radius of Sphere (r/D)	Fraction Small Fines	Potential Debris Volumes (V/D^3)
NEI Recommended Damage Pressures			
PWR Two-Phase Jet (Confirmatory)	7.5	0.25	448
Alternate Damage Pressures			
PWR Two-Phase Jet (Confirmatory)	11.9	0.086	608

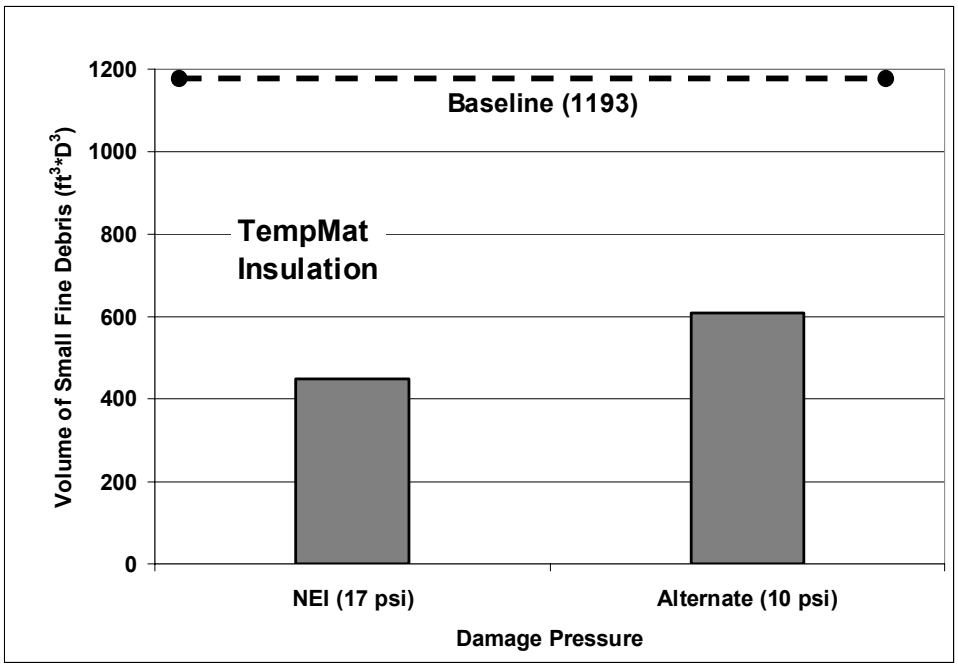

Figure II-5. Potential Volumes of Small Fine Temp-Mat Debris

II.3.1.3 K-Wool Debris

K-wool is also higher density insulation (approximately 10 lb/ft^3) than the LDFG insulation and requires an even higher jet pressure to damage the insulation. The NEI-recommended damage pressure for K-wool is 40 psi. Figure II-6 shows the K-wool

insulation debris fractions for the small fine debris from the AJIT tests. This figure shows only four data points for K-wool, two of which represent tests where no significant damage was noted. The test with the maximum damage had approximately 7.1 percent of the insulation damaged into small fine debris, with much of the remainder of the insulation still contained in the blanket cover and still attached to the target mount. As with the Temp-Mat data, the K-wool damage curve is incomplete because the highest jet pressure tested was that of the NEI-recommended damage pressure. To perform the debris generation integration over the equivalent ZOI sphere, the test data were conservatively extrapolated, as shown in Figure II-6.

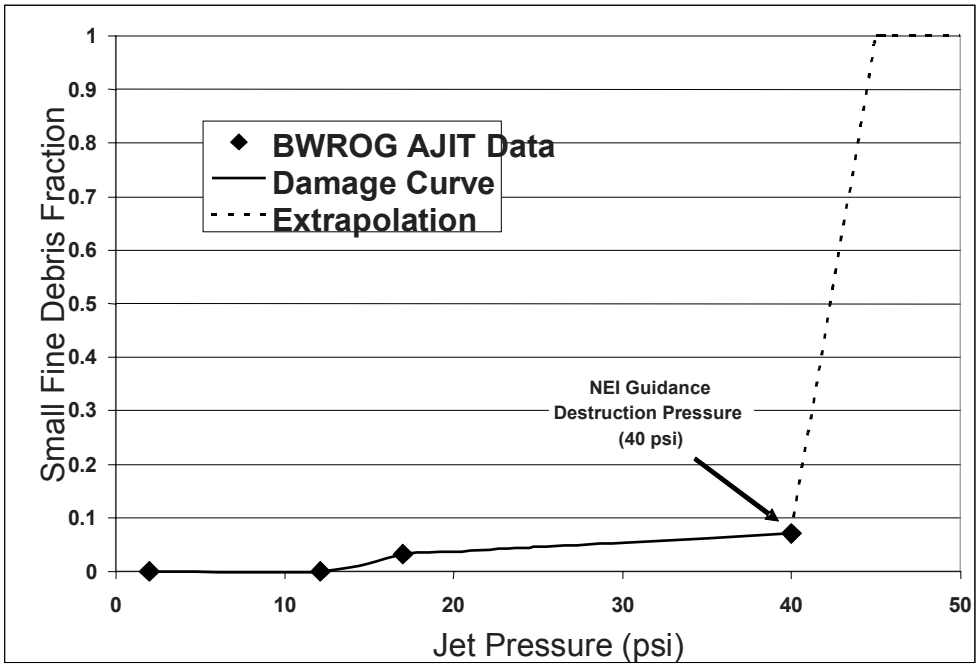

Figure II-6. K-Wool Damage Curve for Small Fine Debris

Table II-4 provides the results of the K-wool debris-size distribution integration over the ZOI. Figure II-7 compares the potential debris volumes and provides an estimate using the baseline guidance (60 percent of $4\pi/3\ (3.8/D)^3$). The lack of debris generation data for a jet pressure higher than the NEI-recommended destruction pressure of 40 psi makes K-wool integration difficult. Therefore, to ensure conservative debris-size integration, it must be assumed that the insulation is completely destroyed at a pressure higher than 40 psi (i.e., the integration herein assumed to be 100 percent at 45 psi). However, this assumption may be overly conservative. For K-wool insulation, the baseline is not conservative with respect to either the NEI guidance damage pressure of 40 psi or the alternate pressure of 17 psi.

Table II-4. Results of Debris-Size Distribution Integration for K-Wool Insulation

Jet Pressure Isobar Volume Calculation	Radius of Sphere (r/D)	Fraction Small Fines	Potential Debris Volumes (V/D^3)
NEI-Recommended Damage Pressures			
PWR Two-Phase Jet (Confirmatory)	4.0	0.92	246
Alternate Damage Pressures			
PWR Two-Phase Jet (Confirmatory)	7.5	0.17	307

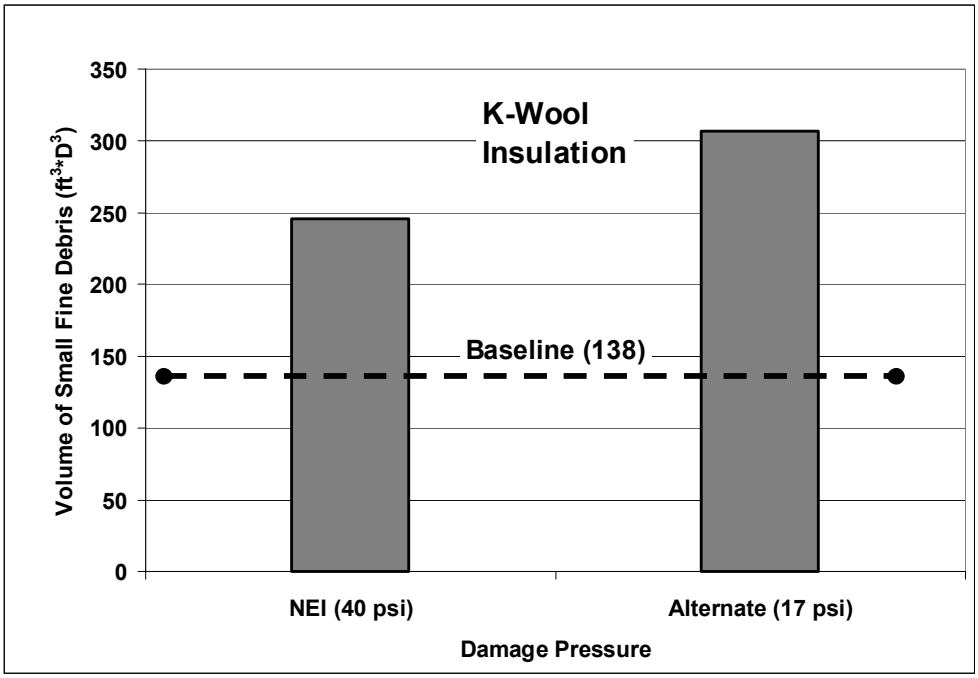

Figure II-7. Potential Volumes of Small Fine K-Wool Debris

II.3.1.4 Correlation between Debris Size and Destruction Pressure

The NEI guidance assumes that it is conservative to adapt the debris-size distribution for NUKON™ to other types of insulations that have a higher destruction pressure than NUKON™ (e.g., Temp-Mat and K-wool). Figure II-8 examines this assumption by comparing the debris generation data for LDFG, Temp-Mat, and K-wool.

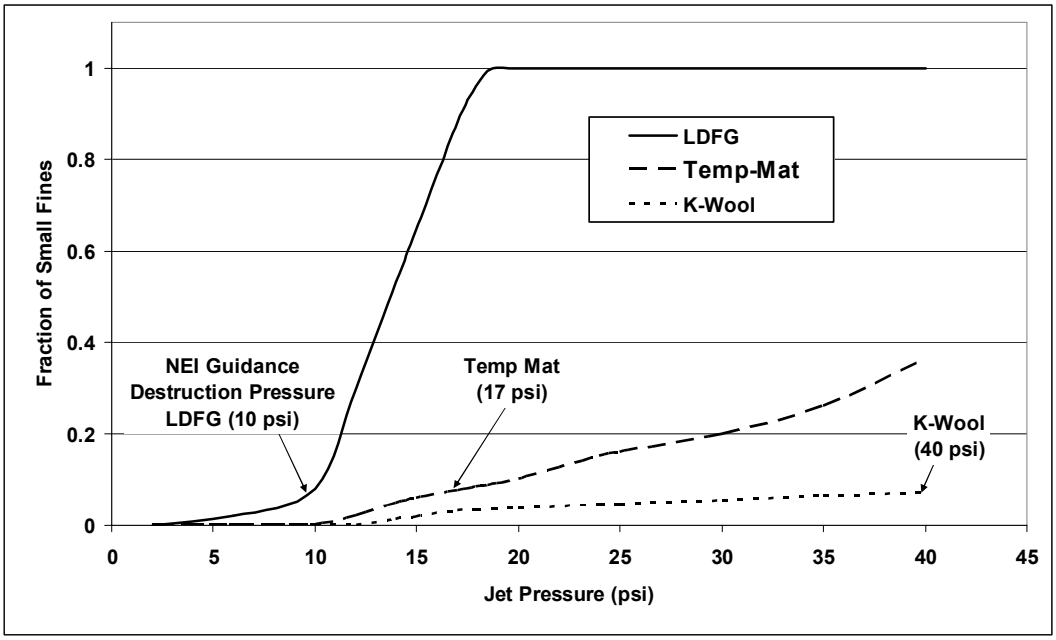

Figure II-8. Comparison of Fibrous Insulation Damage Curves

This damage curve comparison for LDFG, Temp-Mat, and K-wool does seem to support the concept that a higher destruction pressure results in the fractions of small fines becoming increasingly smaller as the destruction pressure increases. Certainly this is the case for Temp-Mat, where the baseline guidance is conservative relative to the integration herein and both the fractions of small fine debris and the potential debris volumes are smaller than the baseline guidance. Although this case is likely true for K-wool as well, it cannot be proven conclusively because of the complete lack of data beyond the NEI-recommended destruction pressure.

II.3.2 RMI Debris

The NEI guidance contains recommendations for three types of RMI insulation:

(1) DARMET®, manufactured by Darchem Engineering, Ltd.

(2) RMI, manufactured by TPI

(3) Mirror®, marketed by Diamond Power Specialty Company (DPSC)

The NEI recommends an assumption that 75 percent of the RMI insulation contained in the equivalent spherical ZOI will be turned into small fine debris. Table II-5 shows the NEI-recommended destruction pressures and the corresponding NEI-recommended radii for those pressures. Note that the ZOI for DARMET® and TPI are quite small compared with the ZOI for DPSC Mirror®.

Table II-5. NEI-Recommended RMI Insulation Destruction Pressures and ZOI Radii

RMI Insulation	Destruction Pressures (psi)	ZOI Radius (r/D)
DARMET®	190 psi	1.3
TPI	190 psi	1.3
DPSC Mirror®	4 psi	21.6

Nearly all the debris generation data used to justify the NEI recommendations came from the BWROG AJIT data (BWROG URG); therefore, the NEI recommendations must be anchored to the insulation types as tested. Besides the BWROG AJIT tests, the U.S. Nuclear Regulatory Commission (NRC) sponsored a single test* using a stainless-steel DPSC Mirror® RMI cassette at the Siemens AG Power Generation Group (KWU) test facility in Karlstein am Main, Germany, in 1994 and 1995 (SEA-95-970-01-A:2, 1996). Table II-6 provides the cassettes and their closures, as tested in the AJIT tests with the cassettes mounted perpendicular to the jet centerline.† All of the cassettes tested had stainless-steel sheaths.

A review of the data indicates that the air jet did not directly penetrate the stainless-steel sheaths; rather, the sheaths disassembled at the seams, such as with rivet failures. Those cassettes secured by stainless-steel bands in addition to latches and strikes generally remained relatively intact. The severity of the damage, in terms of the generation of small fine debris, depends on the degree or ease of disassembling the cassette. However, when considering large-piece debris, all detached cassettes, disassembled or not, become large-piece debris.

Table II-6. BWROG AJIT RMI Insulations Tested

Insulation	RMI Foils Tested	Cassette Closures
DARMET®	Stainless-Steel Foils	Darchem Stainless-Steel Bands and CamLoc® Latches and Strikes
TPI	Aluminum Foils	Latch and Strike Closures
TPI	Stainless-Steel Foils	Latch and Strike Closures
DPSC Mirror®	Aluminum Foils	Latch and Strike Closures
DPSC Mirror®	Stainless-Steel Foils	Latch and Strike Closures
DPSC Mirror®	Stainless-Steel Foils	Latch and Strike Closures and Sure-Hold Band Closures

*The NRC-sponsored test involved a stainless-steel Mirror® cassette mounted directly on a device designed to simulate a double-ended guillotine break, such that the discharge impinged on the inner surface of the RMI target as it would an insulation cassette surrounding a postulated pipe break. This NRC-sponsored test was performed with a high-pressure blast of two-phase water/steamflow from a pressurized vessel connected to a target mount by a blowdown line with a double-rupture disk. This test completely destroyed the cassette into debris that can be considered small fine debris.

†Two tests were conducted, with the cassette mounted parallel to the jet centerline.

II.3.2.1 DARMET®, Manufactured by Darchem Engineering, Ltd.

The NEI-recommended destruction pressure of 190 psi for stainless-steel DARMET®, manufactured by Darchem Engineering, Ltd. and held in place by Darchem stainless-steel bands and CamLoc® latches and strikes, is based on two AJIT tests, Tests 25-1 and 25-2, with jet centerline pressures on target of 190 and 590 psi, respectively. In both of these tests, the cassettes, although deformed, remained intact and attached to the target mount. In effect, the tests did not generate any debris. This result indicates that debris generation requires a pressure greater than 590 psi, with the exception of a cassette mounted over the break, where the jet would enter the inside of the cassette. This scenario would almost certainly result in complete destruction of that cassette. Another possible exception could be a jet approximately parallel to the cassette sheath that could penetrate through the ends—a configuration that has not been tested. It is apparent that the baseline recommendation of assuming that 75 percent of this insulation within a 1.3/D spherical radius becomes small fine debris is conservative.

II.3.2.2 RMI, Manufactured by Transco Products, Inc.

TPI manufactures stainless-steel and aluminum RMI insulation. The NEI guidance recommends a destruction pressure of 190 psi for the TPI RMI. The TPI cassettes tested included both aluminum and stainless-steel foils encased in stainless-steel sheaths secured with latches and strikes (no bands were used). Although the recommended destruction pressure is 190 psi, a small amount of fine debris was noted for jet pressures as low as 10 psi (Test 21-3). On the other hand, only small quantities of fine debris (i.e., less than 0.5 percent) were found for tests with jet pressures as high as 600 psi. Figure II-9 shows the debris generation fractions for TPI stainless-steel RMI small fine debris.

Table II-7 compares potential debris volumes when estimated using the NEI baseline guidance and when acknowledging debris generation at jet pressures as low as 10 psi. As stated above, to obtain actual volumes of debris, the potential volumes must be multiplied by the insulation concentration and again by D^3. For the baseline estimate, the volume associated with a ZOI radius of 1.3/D is multiplied by 75 percent to obtain the baseline potential volume. For the alternate estimate, the ZOI volume out to a jet pressure of 10 psi was multiplied by 0.5 percent to obtain the alternate potential volumes. The application of the alternate pressure results in approximately three times as much small fine debris as using the baseline guidance. However, even these quantities are not very large compared with such insulations as LDFG.

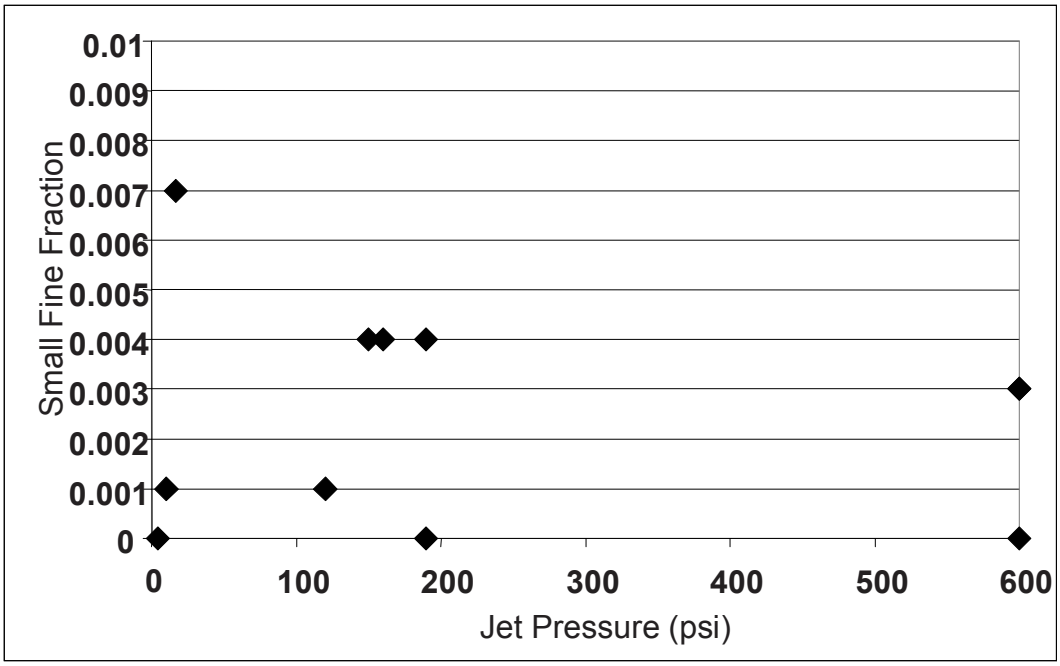

Figure II-9. TPI Stainless-Steel RMI Small-Fine-Debris Fractions

Table II-7. Comparison of TPI Potential Debris Volumes

Guidance	Damage Pressure (psi)	Radius of ZOI (r/D)	Damage Fraction	Potential Volume of Debris (V/D^3)
Confirmatory Recommended Jet Isobar Volumes				
NEI Guidance	190	1.5	0.75	10.6
Alternate	10	11.9	0.005	35.3

However, if the transport of large-piece TPI RMI debris becomes necessary to the strainer blockage evaluation, the use of 190 psi to define the ZOI is totally inadequate. Although the TPI stainless-steel sheaths may effectively contain the foils, their latches and strikes do not effectively keep the cassettes attached to the mounts (or pipes). AJIT Test 21-2, with a jet pressure of only 4 psi, shows the two cassette half sections detached from the target mount (i.e., the cassettes become large-piece debris). At 4 psi, the ZOI radius would be approximately 21.6/D; therefore, numerous cassettes in various degrees of damage would be expected on the breakroom floor. If the transport flow velocities were sufficient to move cassettes, then these cassettes could become a significant problem.

II.3.2.3 DPSC Mirror®, Manufactured by Diamond Power Specialty Company

DPSC manufactures stainless-steel and aluminum RMI insulations marketed as Mirror® insulations. The Mirror® cassettes tested included both aluminum and stainless-steel foils encased in stainless-steel sheaths secured with latches and strikes with or without

Sure-Hold bands. The NEI guidance recommends a destruction pressure of 4 psi for the DPSC Mirror® insulations. The apparent reason that Mirror® cassettes form debris at much lower pressures than does the TPI RMI is the construction of the sheaths (i.e., the cassette integrity depends on strength of the seams).

Figure II-10 shows the debris fractions for the small fine debris from the AJIT tests. In the figure, the small fine debris was correlated as pieces less than 6 in., although the NEI guidance specified RMI small fines as less than 4 in.; therefore, a small measure of conservatism was added to the comparison. Figure II-10 shows six data points for Mirror®, with two of those tests generating very minor quantities of small fines. Note that with the lower pressure test, where the RMI cassette was exposed to a jet pressure of only 2 psi (AJIT Test 18-3), the cassette was still detached from the target mount, leaving two half cassettes on the chamber floor. The test with the largest quantity of small fine debris (AJIT Test 17-1) had only 10.6 percent of the foils turned into pieces less than 6 in., with the remaining foils becoming large-piece debris. The conservative extrapolation shown in Figure II-10 to complete the spherical ZOI debris fraction integration assumes complete destruction at a jet pressure of 130 psi. Note that in the single NRC-sponsored Mirror® debris generation test conducted at the KWU test facility, the test article was completely destroyed.

Table II-8 provides the results of the Mirror® debris-size distribution integration over the ZOI. The potential debris volume of $661/D^3$ is quite low compared with an estimate using the baseline guidance (i.e., 75 percent of $4\pi/3\ (21.6/D)^3$) of $31660/D^3$. Although this insulation is damaged at jet pressures as low as 4 psi, a relatively small amount of small debris is formed at pressures less than approximately 120 psi, and when the debris damage data are applied to the larger ZOI radius of 21.6/D, only a small fraction of the insulation in that sphere becomes small fine debris. For DPSC Mirror® RMI insulation, the assumption in the NEI baseline guidance that 75 percent of the insulation within a 21.6/D ZOI sphere would become debris less than 4 in. in size (i.e., $31{,}660/D^3$) is overly conservative. However, the quantities of large-piece debris, including nearly intact cassettes, could be very large because even 2 psi can detach the cassettes, which could become very important in containments where the transport velocities are high enough to move this heavier debris significantly.

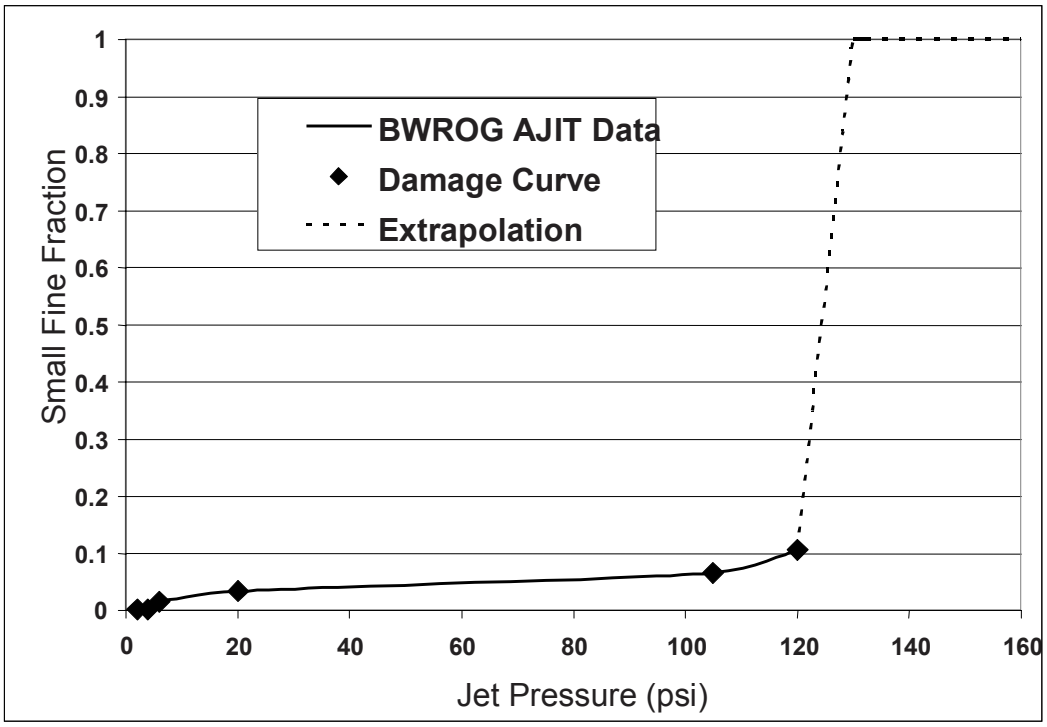

Figure II-10. DPSC Mirror Damage Curve for Small Fine Debris

Table II-8. Results of Debris-Size Distribution Integration for DPSC Mirror® Insulation

Jet Pressure Isobar Volume Calculation	Radius of Sphere (r/D)	Fraction Small Fines	Potential Debris Volumes (V/D^3)
NEI-Recommended Damage Pressures			
PWR Two-Phase Jet (Confirmatory)	21.6	0.016	658

II.3.3 Particulate Insulation Debris

II.3.3.1 Min-K Debris

The NEI baseline guidance recommends the assumption that 100 percent of the Min-K insulation located inside a ZOI defined by the destruction pressure of 4 psi, corresponding to a radius of 21.6/D, becomes small fine debris. The basis for this recommendation is apparently the single Min-K BWROG AJIT debris generation test, Test 9-1. In this test, approximately 70 percent of the Min-K insulation became small fine debris. In fact, most of this debris was not recovered, apparently because it was too

fine.* Based on the extensive damage to this Min-K blanket at 4 psi, it does not seem reasonable to assume that the threshold of damage is 4 psi.

At jet pressures substantially higher than 4 psi, it seems likely that the Min-K would be totally destroyed. At jet pressures less than 4 psi, the damage to Min-K would continue but would decrease in severity until the pressure became insufficient to cause damage. However, that pressure is not known. It is unlikely that the NEI baseline guidance is conservative with respect to the Min-K blanket tested. On the other hand, Min-K insulation protected by a metal jacket secured with steel bands would most likely be substantially less damaged than the unjacketed blanket tested.

II.3.3.2 Calcium Silicate Debris

The NEI baseline guidance recommends the assumption that 100 percent of the calcium silicate insulation located inside a ZOI defined by the destruction pressure of 24 psi (corresponding to a radius of 5.5/D) becomes small fine debris. The OPG debris generation tests (N-REP-34320-10000-R00) were cited to justify the 24-psi destruction pressure. The OPG tests involved impacting aluminum-jacketed calcium silicate insulation targets with a two-phase water/steam jet. The jacketing was secured with stainless-steel bands, and the jacketing seams were typically oriented at 45 degrees from the jet centerline—an orientation that appeared to maximize damage. The OPG data, illustrated in Figure II-11, only cover a limited range of damage pressures (approximately 24 to 65 psi).

The damage curve shown in Figure II-12 was generated by summing all four debris categories in Figure II-11 to obtain the OPG debris fractions shown and then constructing a plausible curve through the data that was conservatively extrapolated at both ends. Table II-9 provides the results of the calcium silicate debris-size distribution integration over the ZOI. Figure II-13 compares the potential debris volumes and provides an estimate using the baseline guidance (100 percent of $4\pi/3\ (5.45/D)^3$). A lower alternate damage pressure results in a larger equivalent spherical ZOI, but a lesser fraction of the debris is damaged into small fine debris. The use of the alternate damage pressures over the NEI-recommended damage pressures for PWR analyses would result in approximately 43 percent more estimated small fine debris. For calcium silicate insulation, the baseline is conservative with respect to both the NEI guidance damage pressure of 24 psi and the alternate pressure of 20 psi.

---

*It was noted that a cloud of debris was observed to exit the test chamber through the exhaust screen and that the venting of the chamber to clear the dust required more than 15 minutes.

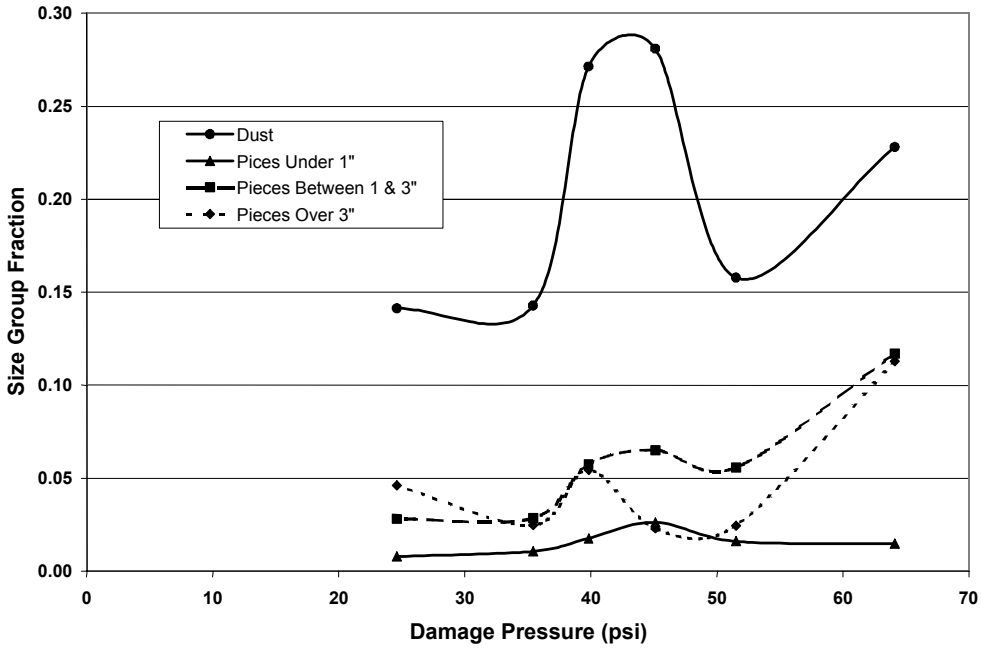

Figure II-11. Debris-Size Distributions for OPG Calcium Silicate Tests

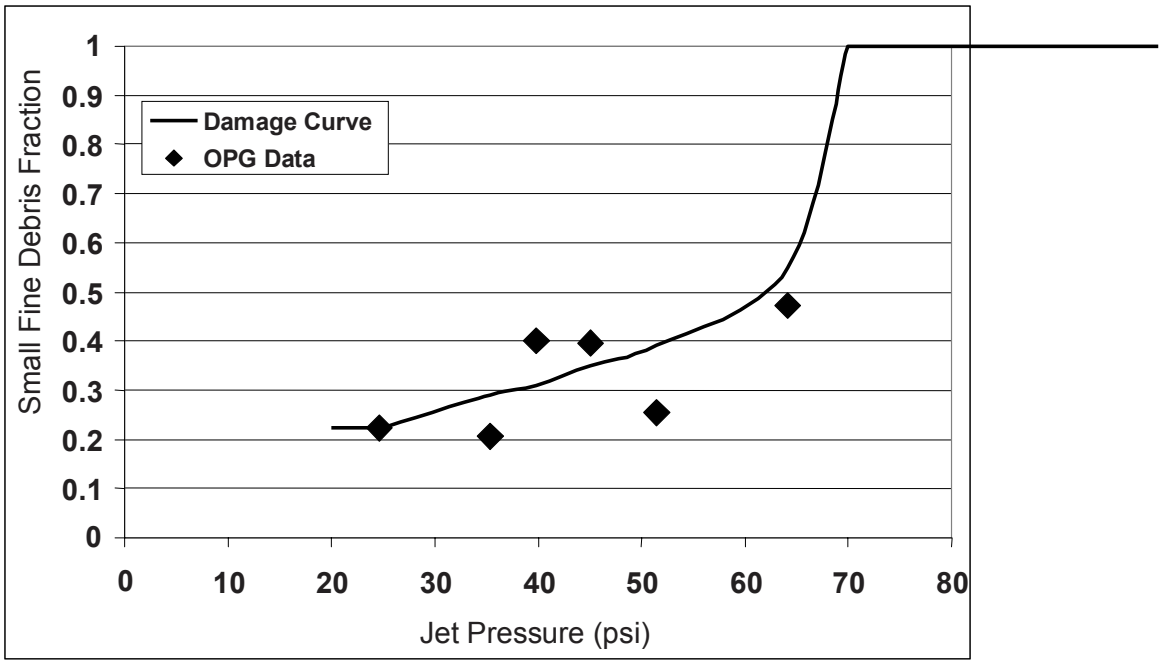

Figure II-12. Calcium Silicate Damage Curve for Small Fine Debris

Table II-9. Results of Debris-Size Distribution Integration for Calcium Silicate Insulation

Jet Pressure Isobar Volume Calculation	Radius of Sphere (r/D)	Fraction Small Fines	Potential Debris Volumes (V/D^3)
NEI-Recommended Damage Pressures			
PWR Two-Phase Jet (Confirmatory)	5.4	0.42	273
Alternate Damage Pressures			
PWR Two-Phase Jet (Confirmatory)	6.4	0.34	372

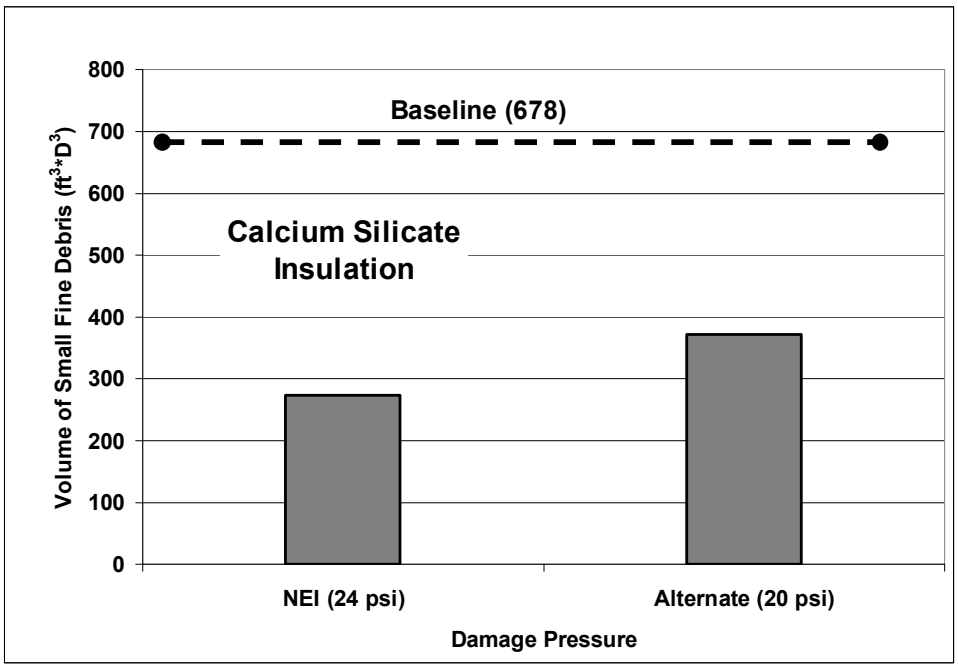

Figure II-13. Potential Volumes of Small Fine Calcium Silicate Debris

The BWROG AJIT tests also contain four tests of calcium silicate with aluminum jacketing secured by four 3/4-in. stainless steel bands; however, these tests indicated that a jet of 150 psi was needed to cause significant damage. The reason that a much higher pressure was needed to cause significant damage in the AJIT calcium tests than in the OPG tests has not been determined, but it likely results from the differences in jacketing thickness, seam orientation, and strength of the bands. Here the destruction pressure depends more on the pressure needed to remove the jacket and expose the insulation than on the pressure required to erode the calcium silicate.

II.4 Summary and Conclusions

Confirmatory research was performed to ascertain whether the NEI recommendations for ZOI destruction pressures and debris fractions would reliably result in conservative estimates for the volumes of debris generated within the ZOI. Specifically, the NEI guidance recommends the assumption that 60 percent of the fibrous and 75 percent of the RMI insulation volume contained within the ZOI become small fine debris for ZOI radii defined by their recommended destruction pressures. The NEI guidance recommends adapting the debris-size distribution for NUKON™ to other types of fibrous insulation that have a destruction pressure higher than that of NUKON™.

Available debris generation data were used to define debris fractions versus jet pressure curves for the insulations examined. Difficulties encountered when correlating these data include aspects of protective jacketing and banding, as well as the variability in insulations. Before the insulation is subjected directly to jet flow forces, the flow must penetrate the protective coverings. Steel bands securing a metal jacket can require a rather high jet pressure to open the jacket before insulation debris is generated. The seam orientation affects the ease with which an edge of the jacket can be peeled back; it appeared that a seam orientation of approximately 45 degrees from the oncoming jet maximizes the potential for jacket opening. The size of the jet nozzle relative to the insulation destruction pressure also affected the quality of debris generation data. If the target insulation had to be placed close to the nozzle to get the required destruction pressure, then the jet pressure became uneven along the length of the target; in fact, in some tests the target ends were likely located outside the influence of the jet. To test insulations with a higher destruction pressure, either larger nozzles or shorter targets are required. The evaluation of debris fractions considers all of these factors.

The ZOI debris fractions and insulation destruction pressures are interdependent; that is, the larger the ZOI, the smaller the fraction of the insulation within the ZOI that becomes small fine debris. Therefore, when the lower alternate pressure is used in the integration process, the resultant debris fraction will be less than that corresponding to the NEI-recommended destruction pressure.

Table II-10 summarizes the results and conclusions regarding relative conservatism of this confirmatory debris generation analyses for the insulations examined. These results are relative to the NEI baseline guidance for the small fine debris size category.

Table II-10. Summary Comparison of Confirmatory and Baseline Potential Debris Volumes

Insulation	Confirmatory Research Result	Relative Conservatism of Baseline Guidance
Fibrous Insulations		
NUKON™	Baseline guidance results compare well with confirmatory results.	Baseline guidance for NUKON™ provides realistic results that are only slightly conservative.
Temp-Mat	Baseline results are approximately twice the confirmatory results (based on limited data).	Baseline guidance is conservative for Temp-Mat insulation.
K-wool	Baseline results are only about half that of the confirmatory results (based on limited data).	Baseline guidance is likely conservative for K-wool, despite the nonconservative comparison with confirmatory analysis. The poor nonconservative comparison results from the extreme extrapolation of data required by the lack of data for pressures greater than the NEI destruction pressure. Still, conservatism cannot be proven with existing data.
RMI Insulations		
DARMET®	No confirmatory analysis for this insulation. Rather, a review of the debris generation data illustrated substantially less small fine debris than would be estimated using the baseline guidance methodology.	Baseline guidance is conservative for DARMET® insulation.
TPI	Baseline results account for only one-third of the confirmatory debris estimate, which includes the small quantities of debris generated at lower pressures but that are neglected when the baseline destruction pressure is used.	Baseline guidance is not conservative, but the quantities of this debris are relatively low; therefore, this nonconservative estimate is not a major issue.
DPSC Mirror®	Baseline results were almost 50 times that of the confirmatory result. The baseline minimum destruction pressure of 4 psi results is a very large ZOI volume, but the damage to the insulation is relatively minor at the lower pressures, thus the large differences in results.	Baseline guidance is conservative for Mirror® insulation.
Particulate Insulations		
Min-K	No confirmatory analysis for this insulation. Rather, the data from the single Min-K debris generation test were examined (i.e., approximately two-thirds of the insulation was turned into fine dust debris at a jet pressure of only 4 psi).	Baseline guidance is not conservative because the one test indicated that substantial damage would occur to Min-K insulation at significantly lower pressures than the destruction pressure of 4 psi and that the damage at 4 psi was extreme.
Calcium Silicate	Baseline results are approximately twice the confirmatory results, even when the lower jet pressure of 20 psi (recommended in NUREG/CR-6808) is considered instead of the baseline destruction pressure of 24 psi.	Baseline guidance appears to be conservative for calcium silicate insulation, but the debris generation data are not sufficient to determine the threshold jet pressure for generating small fine debris (i.e., the threshold destruction pressure could actually be less than the 20 psi alternate pressure used in the confirmatory analysis).

Note the following additional comments:

- The use of the alternate destruction pressure provides some quantification of the uncertainty associated with the selection of the destruction pressures. These uncertainties include the neglect of the tails of the debris damage curves and the uncertainty associated with the potential two-phase effect on debris generation relative to the available air-jet-generated data.
- A comparison of the NUKON™ results with the BWROG URG steam jet model illustrates that the neglect of the tails of the debris damage curve has a larger impact for PWRs than for BWRs (see Figure II-3).
- The NEI guidance recommendation that adapts the debris-size distribution for NUKON™ to other types of fibrous insulation that have a destruction pressure higher than that of NUKON™ has been partially supported (see Figure II-8), although it cannot be conclusively ensured.
- The ZOI for large debris generation in some cases does not correlate with the ZOI for small-fine-debris generation. A case in point is the analysis for TPI RMI, where most of the small fine debris would be generated inside jet pressures of 190 psi, but large debris was generated (in the form of detached cassettes) at pressures as low as 4 psi. Therefore, rather larger quantities of large debris could be formed than were predicted using the baseline guidance ZOI sizes.
- It should be emphasized that the typical debris generation analyses were performed for insulations where the debris generation data were very limited. The data for the LDFG insulations (see Figure II-2) illustrate the potential variability in such data. Therefore, the limited debris generation data cause substantial uncertainty with debris generation estimations.

II.5 References

(NUREG/CR-6762, Volume 3, 2002) C.J. Shaffer, D.V. Rao, and S.G. Ashbaugh, "GSI-191 Technical Assessment: Development of Debris-Generation Quantities in Support of the Parametric Evaluation," LA-UR-01-6640, NUREG/CR-6762, Volume 3, 2002.

(NUREG/CR-6369, 1999) Rao, et al., "Drywell Debris Transport Study: Experimental Work," SEA97-3501-A:15, NUREG/CR-6369, Volume 2, September 1999.

[NEDO-32686, Rev. 0, 1996] "Utility Resolution Guidance for ECCS Suction Strainer Blockage," BWROG, NEDO-32686, Rev. 0, November 1996.

(SEA-95-970-01-A:2, 1996) Zigler, G., et al., "Experimental Investigation of Head Loss and Sedimentation Characteristics of Reflective Metallic Insulation Debris," draft letter report prepared for the U.S. Nuclear Regulatory Commission, SEA No. 95-970-01-A:2, May 1996.

(N-REP-34320-10000-R00, 2001) Ontario Power Generation, "Jet Impact Tests—Preliminary Results and Their Applications," N-REP-34320-10000-R00, April 2001.

(ANSI/ANS-58.2, 1988) American National Standard/American Nuclear Society: "Design Basis for Protection of Light Water Nuclear Power Plants Against the Effects of Postulated Pipe Rupture," ANSI/ANS-58.2-1988, October 1988.